Published as: *Nat Biotechnol*. 2009 June ; 27(6): 567–571.

Efficient siRNA Delivery into Primary Cells by Peptide Transduction-dsRNA Binding Domain (PTD-DRBD) Fusion Protein

Akiko Eguchi[1,2,3], **Bryan R. Meade**[1,2], **Yung-Chi Chang**[4], **Criag T. Fredrickson**[2], **Karl Willert**[2], **Nitin Puri**[5], and **Steven F. Dowdy**[1,2,*]

[1]Howard Hughes Medical Institute, UCSD School of Medicine, 9500 Gilman Drive, La Jolla, CA 92093, USA

[2]Department of Cellular & Molecular Medicine, UCSD School of Medicine, 9500 Gilman Drive, La Jolla, CA 92093, USA

[3]Japan Society for the Promotion of Science, UCSD School of Medicine, 9500 Gilman Drive, La Jolla, CA 92093, USA

[4]Department of Pediatrics, UCSD School of Medicine, 9500 Gilman Drive, La Jolla, CA 92093, USA

[5]Life Technologies, 2150 Woodward St., Austin, TX 78744, USA

SUMMARY

Short interfering RNA (siRNA) induced RNA interference (RNAi) responses allow for discovery research and performing large scale screening1-5; however, due to their size and anionic charge, siRNAs have no bioavailability to enter cells4,5. Current approaches fail to deliver siRNAs into a high percentage of primary cells in a non-cytotoxic fashion. Here we report an efficient siRNA delivery approach that utilizes a Peptide Transduction Domain-dsRNA Binding Domain (PTD-DRBD) fusion protein. DRBDs bind to siRNAs with high avidity, masking the siRNA negative charge and allow for PTD-mediated cellular uptake. PTD-DRBD delivered siRNAs induced rapid RNAi responses in a non-cytotoxic manner in the entire cell population of primary and transformed cells, including T cells, HUVECs and hESCs. Whole genome microarray analysis showed minimal transcriptional changes by PTD-DRBD and we did not detect any innate immune responses in PBMCs. Thus, PTD-DRBD mediated siRNA delivery allows efficient RNAi manipulation of difficult primary cell types.

*Correspondence should be addressed to: sdowdy@ucsd.edu.

AUTHOR CONTRIBUTIONS

A.E., B.M. designed, purified PTD-DRBD and performed RNAi experiments. Y.-C.C performed PBMC experiments. C.T.F. performed hESC culture. K.W. supervised hESC culture. N.P. provided siRNAs reagents. S.F.D supervised and analyzed data. A.E., S.F.D. contributed to writing the manuscript, and all authors discussed and refined the manuscript.

Supplementary data

Please see attached supplementary figures.

COMPETING INTERESTS STATEMENT

The authors declare competing financial interests.

RNAi has become a corner-stone for directed manipulation of cellular phenotypes, mapping and screening genetic pathways, discovering and validating therapeutic targets, and has significant therapeutic potential1-5. However, due to their ∼14,000 Dalton (Da) size and extensive negative (anionic) charge, simply stated, siRNAs are macromolecules with no ability to enter cells4,5. In fact, naked siRNAs fail to enter unperturbed cells or induce an RNAi response, even at millimolar concentrations4. Consequently, significant attention has been focused on devising siRNA cellular delivery approaches, including particle formation by cationic lipids, cholesterol, condensing polymers, antibody-protamine fusions and siRNA encapsulation in liposomes1-5. However, these siRNA delivery approaches perform best on adherent tumor cells and poorly on primary cells and non-adherent cell types, thereby severely limiting the cell types that can be used for discovery research and large scale RNAi screening. Consequently, there is a significant need for a siRNA delivery approach that: 1) targets the entire cell population of all primary and tumorigenic cell types, 2) is non-cytotoxic, and 3) is independent of siRNA sequence.

In developing a siRNA delivery strategy, we started with the proven macromolecular delivery properties of cationic Peptide Transduction Domain (PTD) delivery vehicle (also termed Cell Penetrating Peptide [CPP]), such as TAT, 8×Arg, and Antp, that have been shown to deliver a wide variety of cargo into primary cells, into most, if not all, tissues in pre-clinical models and are currently being tested in multiple clinical trials6. Cationic PTDs are rapidly taken up into cells by macropinocytosis, a specialized form of fluid phase uptake that all cells perform7,8. However, conjugation of cationic PTDs (6-8 positive charges) to anionic siRNAs (∼40 negative charges) results in charge neutralization, inactivation of the PTD, aggregation/precipitation, and cytotoxicity with limited siRNA entry into the cells9,10. To circumvent PTD charge neutralization (inactivation), we generated a TAT PTD fusion protein with a single dsRNA Binding Domain (PTD-DRBD) that binds the siRNA with high avidity ($K_D \sim 10^{-9}$) and thereby masks its negative charge11-13. DRBDs are small, ∼65 residue domains that specifically binds ∼12-16 bp of the dsRNA backbone on 90° surface quadrants of the dsRNA helix, resulting in four DBRDs encompassing a single siRNA (4:1 ratio) (Fig. 1a) (Supplementary Fig. 1).

To determine the ability of PTD-DRBD fusion proteins to deliver siRNAs, we generated a human H1299 lung adenocarcinoma dGFP/dDsRed reporter cell line that allowed for direct determination of the magnitude of a single cell RNAi response and hence, the percentage of cells undergoing a RNAi response. H1299 dGFP/dDsRed reporter cells were treated with PBS (mock), PTD-DRBD plus control control (Con1, Con2) siRNAs or PTD-DRBD plus one of two sequence-independent GFP (GFP1, GFP2) siRNAs and analyzed by flow cytometry for GFP knockdown at 24 h (Fig. 1b, left panel). PTD-DRBD delivery of GFP specific siRNAs resulted in a significant GFP knockdown with little to no alteration of the internal DsRed control. Similar RNAi responses were induced with 3 additional GFP siRNAs delivered by PTD-DRBD (data not shown). All controls (non-specific control siRNAs, PTD delivery peptide only) failed to induce a RNAi response. PTD-DRBD mediated siRNA delivery also resulted in a significantly stronger RNAi response compared to lipofection delivered siRNAs (Fig. 1b, right panel). Importantly, we detected little to no alteration of cell viability in PTD-DRBD:siRNAs treated cells, whereas lipofection resulted in varying levels of cytotoxicity (Supplementary Fig. 2). Single cell flow cytometry analysis

of PTD-DRBD:GFP siRNA treated cells showed that the entire cellular population was undergoing a maximal RNAi response at 24 h that was maintained at 48 h (Fig. 1c,d). In contrast, lipofection delivered siRNAs induced a partial penetrant RNAi response with ∼20% of cells unresponsive (Fig. 1c,d). Kinetic analysis over 8 days in dividing H1299 cells showed a slow decay of the RNAi response starting 3 days after PTD-DRBD:GFP siRNA treatment that was similar to the lipofection mediated RNAi decay kinetics (Fig. 1e). Similar results were obtained in primary human fibroblasts, keratinocytes, macrophage, melanoma and glioma cells containing integrated GFP reporter genes (Supplementary Fig. 2). To circumvent the RNAi decay curve, we re-treated dividing H1299 cells on days 3 and 6 with PTD-DRBD:GFP siRNAs resulting in maintenance of the extent and magnitude of the GFP RNAi response (Fig. 1f).

We next targeted endogenous GAPDH mRNA by PTD-DRBD mediated RNAi. Treatment of H1299 cells with one of two sequence-independent GAPDH siRNAs delivered by PTD-DRBD resulted in a GAPDH RNAi response that was first detected by qRT-PCR at 6 h post-addition and reached a maximal RNAi response by 12 h (Fig. 1g,h). In contrast, all PTD-DRBD negative controls failed to induce a GAPDH RNAi response. Impressively, PTD-DRBD mediated delivery of GAPDH1 siRNA resulted in a near maximal RNAi response by 6 h, significantly ($P<0.001$) earlier than control lipofection delivery of the same GAPDH siRNAs (Fig. 1g), suggesting that PTD-DRBD delivered siRNAs rapidly enter the cytoplasm and are loaded into RISC. To determine if PTD-DRBD mediated siRNA delivery caused any cellular alterations, we examined the transcriptome of treated cells. Whole genome microarrays were probed with total mRNA from PTD-DRBD GAPDH siRNA treated H1299 cells at 12 h and 24 h (Fig. 1i). Using a 1.6× fold increase/decrease filter (blue line) of cellular mRNAs, we detected a dramatic reduction in the target GAPDH mRNA along with a limited number of both up and down regulated genes. The up regulated genes were reduced in numbers and to nearly background 1.6× levels at 24 h, while the down regulated genes increased slightly in numbers and maintained a similar magnitude at 24 h (Fig. 1i). None of these genes are present in either an innate immune response pathway or congregate into a specific genetic pathway. In contrast, lipofection treated cells showed both a dramatic increase in both the total number of genes altered and the magnitude of the increase (Fig. 1j). In addition, the numbers of genes affected increased between 12 h and 24 h, suggesting that lipofection of siRNAs into cells results in a substantial alteration to the transcriptome and may thereby caveat interpretation of experimental outcomes. Moreover, lipofection mediated GAPDH specific knockdown was significantly smaller than PTD-DRBD mediated knockdown. Taken together, these observations demonstrate that PTD-DRBD mediated siRNA delivery efficiently targets the entire cellular population in the absence of cytotoxicity.

Due to inefficient siRNA delivery and associated cytotoxicities, RNAi manipulation of T cells remains problematic. Therefore, we focused on a notoriously difficult cell type to delivery siRNAs into, namely tumorigenic Jurkat T cells. Jurkat T cells containing an integrated GFP reporter gene were treated with GFP siRNA plus either PTD-DRBD or one of two lipofection reagents (Lipofection-2000 and RNAiMAX) at optimal concentrations and analyzed by flow cytometry for GFP knockdown at various time points (Fig. 2a). PTD-DRBD delivery of GFP specific siRNAs into Jurkat T cells resulted in a strong GFP RNAi

response in the entire population of Jurkat T cells. In comparison, both lipofection reagents induced limited RNAi responses. Moreover, PTD-DRBD delivered GAPDH siRNA into Jurkat T cells resulted in a strong GAPDH RNAi response as measured by qRT-PCR, whereas the two lipofection reagents performed poorly (Fig. 2b). We next treated primary murine T cells with PTD-DRBD plus CD4 specific siRNAs and assayed for CD4 cellular levels by flow cytometry (Fig. 2c, left panel). The entire CD4 cellular population had undergone an RNAi response at 24 h, whereas control siRNAs did not alter CD4 levels. Similarly, PTD-DRBD mediated delivery of CD8 specific siRNAs into primary T cells resulted in a CD8 specific RNAi response with no change in CD4 levels (Fig. 2c, middle panel). Consistent with these observations, we detected PTD-DRBD CD4 and CD8 specific RNAi responses by qRT-PCR at 12 and 24 h ($P<0.05$) (Fig. 2d). Importantly, both flow cytometry and qRT-PCR analyses of internal control CD90 receptor showed little to no alteration in either PTD-DRBD CD4 or CD8 siRNA treated T cells (Fig. 2c,d). In contrast, we were unable to detect any RNAi responses by lipofection of primary T cells (data not shown).

Primary human umbilical vein endothelial cells (HUVEC) are an important cell type for large scale RNAi screen; however, lipofection delivery of HUVECs results in both poor siRNA delivery and cytotoxicity. We targeted endogenous GAPDH mRNA by PTD-DRBD mediated RNAi. Treatment of primary HUVECs with one of two sequence-independent GAPDH siRNAs delivered by PTD-DRBD resulted in a GAPDH RNAi response that was first detected by qRT-PCR at 6 h post-addition and reached a maximal RNAi response by 12 h ($P<0.01$) (Fig. 2e). In contrast, all PTD-DRBD negative controls failed to induce a GAPDH RNAi response. Consistent with the observations in H1299 cells above, PTD-DRBD mediated delivery of GAPDH1 siRNA resulted in a maximal RNAi response by 6 h (Fig. 2e). Importantly, we detected little to no alteration of HUVEC cell viability in PTD-DRBD:siRNA treated cells compared to mock treated control cells (Fig. 2f). In contrast, we were unable to lipofect siRNAs into HUVECs without inducing significant levels of cytotoxicity (Fig. 2f).

Human Embryonic Stem Cells (hESCs) have great potential to treat human disease14; however, manipulation of hESCs into specific cell lineages by RNAi requires protocols that target the entire cell population in a non-cytotoxic manner. We first tested the ability of PTD-DRBD to deliver siRNAs into H9 hESCs stably expressing GFP. Consistent with the observations above, PTD-DRBD mediated delivery of GFP siRNAs induced a marked GFP RNAi response throughout the hESC colony (Fig. 3a, circled area). We next tested the ability of PTD-DRBD mediated siRNA delivery to affect the fate of hESCs. The Oct4 (POU5F1) transcription factor is required to maintain hESC pluripotency and Oct4 RNAi knockdown results in hESC cell cycle exit and differentiation14. Treatment of HUES9 hESCs with PTD-DRBD plus Oct4 siRNA resulted in both an Oct4 specific knockdown followed by a reduced growth rate and cell cycle exit indicative of pluripotency loss and initiation of differentiation (Fig. 3b,c). In contrast, both mock and PTD-DRBD plus control siRNA did not alter hESC cellular morphology, growth kinetics or Oct4 expression levels.

Pluripotent hESCs express multiple cell surface markers, including Stage-Specific Embryonic Antigen-4 (SSEA-4)15. During differentiation into endoderm, hESCs decrease

SSEA-4 expression, stop dividing, increase in size and subsequently express the GATA6 differentiation transcription factor16. PTD-DRBD delivered Oct4 siRNA resulted in loss of Oct4 expression by day 2 with continued SSEA-4 expression (Fig. 3d). However, by 10 days post-treatment, Oct4 siRNA treated cells had lost expression of SSEA-4 and induced expression of the GATA6 endoderm specific transcription factor (Fig. 3e). In contrast, mock and PTD-DRBD plus control siRNA treated hESCs did not induce differentiation or alter hESC marker expression. Similar results were obtained by simultaneous PTD-DRBD mediated knockdown of Oct4 and Nanog (data not shown). siRNAs have been shown to stimulate activation of Toll-Like Receptors-3, -7, -8 (TLR) to induce innate immune responses17. However, PTD-DRBD mediated delivery of immunostimulatory siRNAs failed to activate IFN-α or TNF-α responses in primary human peripheral blood mononuclear cells (PBMCs) above background levels (Fig. 3f,g). Taken together, these observations demonstrate the ability of PTD-DRBD to deliver siRNA and rapidly induce RNAi responses in three important and difficult to deliver cell types: T cells, HUVECs, and hESCs.

siRNA-induced RNAi has great potential to treat human disease, including nasal delivery to treat virus infection18; however, in vivo siRNA delivery remains problematic1-5. Based on the efficient PTD-DRBD mediated siRNA delivery we observed in primary cell culture systems, we quantified the ability of PTD-DRBD to deliver siRNAs and induce an RNAi response using an intranasal in vivo transgenic Luciferase reporter mouse model19. Transgenic ROSA26 mice stably expressing tissue restricted luciferase in the nasal and tracheal passage were live animal imaged for Luciferase expression then randomized into groups (Fig. 3h,i). Luciferase mice were then treated intranasally with PBS, PTD-DRBD plus Luc siRNA or control siRNA and monitored daily for 15 days for luciferase expression. Control PBS and PTD-DRBD control siRNA mice showed no change in luciferase expression over the course of the experiment. In contrast, PTD-DRBD delivered Luc siRNA showed extensive reduction of luciferase expression throughout the nasal and trachea at day 1 and gradually recovered luciferase expression by day 15 (Fig. 3h,i). These observations demonstrate the ability of PTD-DRBD mediated siRNA delivery to induce a specific RNAi response to a quantifiable target protein in reporter mouse models in vivo.

siRNA induced RNAi responses are a key experimental procedure for manipulation of cell biology, dissection of genetic pathways, target validation and have great potential for therapeutic intervention. However, due to their macromolecular size (~14,000 Da) and strong anionic charge, siRNAs have limited to no ability to enter cells on their own, even at millimolar concentrations. Indeed, siRNA delivery has become the rate-limiting barrier to efficient cell culture, pre-clinical and clinical usage of siRNA therapeutics1-5. Consequently, significant effort has been placed on devising efficient siRNA delivery approaches. While current siRNA delivery approaches have merit, they generally fail to target the entire population of cells or a high percentage of cells, especially primary cells, and often result in varying levels of cytotoxicity and alterations in cell biology. In contrast, the PTD-DRBD siRNA delivery approach described here fulfills many of the criteria for an efficient siRNA delivery system into primary cells. PTD-DRBD delivered siRNAs and induced RNAi responses in the entire population of three difficult to deliver primary cell types (T cells, HUVECs, and hESCs) in a rapid and non-cytotoxic fashion. DRBDs bind to dsRNAs (siRNAs) independent of sequence composition and therefore, in theory, PTD-

DRBD can deliver any siRNA into cells. Lastly, the intranasal knockdown of luciferase in vivo begins to demonstrate an in vivo potential of PTD-DRBD mediated siRNA delivery; however, significantly more in vivo work needs to be performed to ascertain the full extent of in vivo utility. In summary, PTD-DRBD has broad implications for the scientific community in RNAi basic research, target screening and potential therapeutic applications.

METHODS

PTD-DRBD Fusion Protein Construction, Design and Purification

pPTD-DRBD was constructed by PCR cloning of PKR DRBD-1 into a modified pTAT vector8 resulting in TAT-TAT-HA-TAT-DRBD-6xHis (Supplementary Fig. 1). The HA epitope tag was used to follow the protein by immunoblot analysis and the 6xHis tag was used for purification over the first column, Ni-NTA. PTD-DRBD expression utilized BL21 codon plus (DH3) E.coli (Strategene) cells were transformed with pPTD-DRBD, cultured at 37°C in LB, then at 25°C for 12 h after induction with 400 μM IPTG. Cells were recovered by centrifugation for 5 min at 4,500 g, sonicated in Buffer A (20 mM Hepes [pH 7.5], 500 mM NaCl, 5 μg/ml Aprotinin, 1 μg/ml Leupeptin, 0.8 mM PMSF) plus 20 mM imidazole and soluble protein isolated by centrifugation for 15 min at 50,000 g. PTD-DRBD was purified by passage over a Ni-NTA column (Qiagen), followed by loading onto a Mono-S AKAT FPLC in Buffer B (50 mM Hepes [pH 7.5], 20 mM NaCl, 5% glycerol) and eluted in Buffer C (Buffer B plus 1.5 M NaCl). Purified PTD-DRBD was desalted (PD-10) into PBS-10% glycerol, and stored at −80°C. EGFP-PEST (dGFP) or DsRed-PEST (dDsRed) lenti-viruses were constructed using pCSC-SP-CW-EGFP-PEST or pCSC-SP-CW-DSRED20 and pd2EGFP-N1- (destabilized GFP; BD clontech) or pDsRed-Express-DR (destabilized DsRed; BD clontech).

Cell Culture Conditions

H1299, HaCaT keratinocytes, HFF primary human fibroblasts, B16F0 melanoma cells were cultured in 10% FBS-DMEM, antibiotics. T98G glioblastoma cells were cultured in 5% FBS-MEM, antibiotics. HUVEC cells were cultured in EGM-2 MV BulletKit (Lonza). Jurkat T cells were cultured in 10% FBS-RPMI, antibiotics. THP-1 macrophage were grown in 10% FBS-RPMI plus 1 mM sodium pyruvate, 4.5 g/L glucose, 50 μM β-mercaptoethanol, antibiotics. Primary murine T cells were recovered from mouse spleens by MACS (Miltenyi Biotec), activated with anti-CD3ε antibody for 1 day and cultured in 10% FBS-RPMI plus 2 mM L-Glutamine, 55 μM β-mercaptoethanol, 20 ng/mL IL2. The hESC line HUES9 was kindly provided by D. Melton (HHMI, Harvard University) and H9 hESCs were obtained from WiCell. H9 hESCs were grown in 20% knockout serum-DMEM-F12 plus 55 μM β-mercaptoethanol, NEAA, Gluta-Max, 4 ng/ml bFGF, antibiotics on murine fibroblast feeder layer. HUES9 hESCs were grown in HUES media (10% knockout serum-DMEM plus 10% Plasmonate, 55 μM β-mercaptoethanol, NEAA, Gluta-Max, 4 ng/ml bFGF, antibiotics) without murine fibroblast feeder layer in media preconditioned for 24 h on murine fibroblasts. Destabilized GFP (dGFP) and DsRed (dDsRed) proteins have ∼2 h and ∼12 h half-lives, respectively, significantly shorter than their wild type parental proteins (>24 h) and therefore were used as RNAi reporter targets. dGFP and dDsRed expressing cells were

generated by infection with VSVG expressing dGFP and/or dDsRed (BD Clontech) lentivirus. VSVG-dGFP and/or VSVG-dDsRed infected cells were isolated by FACS.

PTD-DRBD siRNA Delivery into Cells

A typical PTD-DRBD siRNA delivery reaction mixed 10 μl of 1-5 μM siRNA in water with 10 μl of 10-50 μM PTD-DRBD in PBS-10% glycerol plus 4 μl PBS-10% glycerol on ice for 30 min, diluted 1:5 in media and added to 6×10^4 cells/well in 48 well plate for 1-6 h with final siRNA concentrations between 100-400 nM. Cells were then washed with trypsin or washed in 58 μg/ml heparin sulfate plus media for 10 min to remove extracellular PTD-DRBD:siRNA, followed by addition of fresh media plus FBS. For primary T cells, Jurkat, Namalwa, THP-1 suspension cells, 2×10^5 cells were treated with 100-400 nM siRNA:PTD-DRBD for 1 h in media plus 10-20% Q-serum (5 ml FBS + 1 ml Source 30Q resin [Amersham Bioscience], 30 min at RT on mixing platform, followed by 0.22 μm filtration), washed 2x with media, followed by addition of fresh complete media. For H9 and HUES9 hESCs, 6.6×10^5 cells were treated with 200-400 nM siRNA-PTD-DRBD for 1 h in serum-free media with no feeder layer, followed by 5 hr in serum-free media on fibroblast feeder layer, then 24 h with full HUES media plus serum. For control siRNA lipofections, cells were treated with a dose curve that yielded the highest RNAi response with 100 nM siRNA in Lipofectamine-2000 (Lipofection)(Invitrogen) or 10-50 nM siRNA in Lipofectamine-RNAiMAX (Lipofection 2) (Invitrogen) per the manufacturer's instructions. siRNAs sequences used in this study: EGFP1 (Ambion pre-designed siRNA), EGFP2 (Ambion #4626 Silencer GFP), GAPDH1 (Ambion #4626), GAPDH2 (Ambion #4605), Oct4 (Ambion pre-designed), Nanog (Ambion pre-designed), Sox2 (Ambion pre-desgined) and Silencer Negative (control 1) (Ambion #4611G); luciferase (control 2) (Dharmacon #D-001400-01-20), DsRed (Ambion pre-designed), β-gal17 (Dharmacon).

Immunoblotting, RT-PCR and microarrays

6×10^4 cells/well in 48 well were recovered with trypsin/EDTA, whole cell lysates were prepared in RIPA buffer (1% TritonX-100, 1% Sodium Deoxycholate, 40 mM Tris-HCl, 150 mM NaCl, 0.2% SDS, 5 μg/ml Aprotinin, 1 μg/ml Leupeptin, 0.8 mM PMSF) for 30 min on ice, clarified by centrifugation and proteins resolved by 10% SDS-PAGE. Immunoblot analyses were performed on PVDF membranes blocked in 4% skim milk, PBS-T (0.05% PBS, Tween20) for 1 h at RT, reacted with anti-Oct4 (Santa Cruz), anti-GAPDH (Santa Cruz) and anti-α-tublin (Sigma) antibodies overnight at 4°C, then washed and exposed to HRP conjugated anti-IgG (Santa cruz) antibodies and detected by ECL (Pierce). For GAPDH mRNA TaqMan RT-PCR (Applied Biosystems), 6×10^4 dGFP-H1299 cells/well in 48 well plate were treated as described above with 400 nM GAPDH, control Silencer Negative or control Luciferase siRNA and total RNA isolated at 6, 12, 24, 36, 72 and 96 h post-addition. 5×10^4 HUVEC cells/well in 48 well plate were treated as described above with 400 nM GAPDH, control Silencer Neagtive or control GFP siRNA and total RNA isolated at 6, 12 and 24 h post-addition. cDNA was synthesized using Oligo-dT and GAPDH mRNA expression was detected using TAQ-MAN probe (Ambion) on 7300 Real time PCR system (Applied Biosystems). Mean values normalized to β2 microglobulin and reported as percent of mock GAPDH control, error bar indicates s.d., all experiments performed in triplicate. For whole genome microarrays analysis, 6×10^5 H1299 cells/well in 6 well plate

were treated as described above with 400 nM GAPDH or PBS. Total RNA was isolated at 12 and 24 h post-addition, and used to probe whole genome microarrays (Illumina) at Biogem core (UCSD).

Immunohistochemistry and Flow Cytometry Analysis

Cells were fixed with 4% paraformaldehyde for 30 min at RT, permeabilized in 0.1% TritonX100-PBS for 15 min at RT, blocked in 3% skim milk-PBS for 30 min at RT, then reacted with anti-Oct4 (Santa Cruz), anti-SSEA4 (Santa Cruz) and anti-GATA6 (Santa Cruz) antibodies in 0.1% BSA-PBS overnight at 4°C. Cells were washed and reacted with either Alexa488 or Alexa594 conjugated anti-IgG (Molecular Probes) for 30 min at RT. DNA was counter stained with Hoechst 33342 (Molecular Probes). Cells were analyzed by confocal microscopy (Olympus Flouview. For flow cytometry, 1×10^4 dGFP and/or dDsRed positive cells were analyzed on a FACScan (BD Biosciences).

IFN-α and TNF-α analyses

Human Peripheral blood mononuclear cells (PBMCs) were isolated from healthy donors by standard density gradient centrifugation with Ficoll-Paque PLUSTM (Amersham Biosciences) at 2000 rpm for 20 min at 20°C. To remove platelets, PBMCs were washed 4x in 50 ml PBS, centrifuged at 1500 rpm for 8 min at 4°C. 8×10^5 freshly isolated PBMCs were treated as described above with 100 nM β-gal siRNA17 plus either PTD-DRBD or Lipofection and seeded into 96 well-plate (4×10^5 cells/well). As a positive control, PBMCs were treated with 10 μg/ml Imiquimod for IFN-α induction and 10 μg/ml LPS for TNF-α induction. Culture supernatants were collected at 4 h and 24 h post-addition, and assayed for IFN-α and TNF-α by ELISA (R&D systems).

Intranasal PTD-DRBD siRNA in vivo delivery

Transgenic ROSA26 loxP-Stop-loxP Luciferase mice19 (Jackson Labs) were inoculated intratracheally with 30 μl of 3 mg/ml TAT-Cre8 to turn uciferase gene by removal of a loxP-STOP-loxP DNA transcriptional terminator genetic element. After 3 months, D-Luciferin (150 mg/kg) was administrated intraperitoneally and luciferase expression monitored by live animal imaging (IVIS-100 Xenogen) for 5-15 min post-luciferin injection, twice daily per mouse (Day 0). Following this baseline measurement, mice were randomized into groups (n=3) and inoculated intranasally with 60 μl (30 μl/nostril) of PTD-DRBD plus 750 pmol Luc siRNA or control GFP siRNA or PBS:MEM (1:1) (mock) control. Luciferase expression was monitored by IVIS imaging, twice daily per mouse each day for 15 days.

Statistical analysis

Data are expressed as mean ± s.e.m. as indicated and compared by two-tailed t tests. We assign statistical significance at $P < 0.05$.

Supplementary Material

Refer to Web version on PubMed Central for supplementary material.

ACKNOWLEDGEMENTS

We thank V. Nizet (UCSD) for PBMCs. A.E. was funded by a JSPS Research Fellowships for Young Scientists. This work was supported by a Specialized Center of Research (SCOR) grant from the Leukemia & Lymphoma Society (S.F.D.), the Elsa U. Pardee Foundation (S.F.D.) and the Howard Hughes Medical Institute (S.F.D.).

REFERENCES

1. de Fougerolles A, Vornlocher HP, Maraganore J, Lieberman J. Interfering with disease: a progress report on siRNA-based therapeutics. Nat. Rev. Drug Discov. 2007; 6:443–453. [PubMed: 17541417]
2. Kim DH, Rossi JJ. Strategies for silencing human disease using RNA interference. Nat. Rev. Genet. 2007; 8:173–184. [PubMed: 17304245]
3. Bumcrot D, Manoharan M, Koteliansky V, Sah DW. RNAi therapeutics: a potential new class of pharmaceutical drugs. Nat. Chem. Biol. 2006; 2:711–719. [PubMed: 17108989]
4. Whitehead KA, Langer R, Anderson DG. Knocking down barriers: advances in siRNA delivery. Nat. Rev. Drug. Discov. 2009; 8:129–138. [PubMed: 19180106]
5. Behlke MA. Chemical modification of siRNAs for in vivo use. Oligonucleo. 2008; 18:305–319.
6. Gump JM, Dowdy SF. TAT transduction: the molecular mechanism and therapeutic prospects. Trends Mol. Med. 2007; 13:443–448. [PubMed: 17913584]
7. Nakase I, et al. Cellular uptake of arginine-rich peptides: roles for macropinocytosis and actin rearrangement. Mol. Ther. 2004; 10:1011–1022. [PubMed: 15564133]
8. Wadia JS, Stan RV, Dowdy SF. Transducible TAT-HA fusogenic peptide enhances escape of TAT-fusion proteins after lipid raft macropinocytosis. Nat. Med. 2004; 10:310–315. [PubMed: 14770178]
9. Turner JJ, et al. RNA targeting with peptide conjugates of oligonucleotides, siRNA and PNA. Blood Cells Mol. Dis. 2006; 38:1–7. [PubMed: 17113327]
10. Meade BR, Dowdy SF. Enhancing the cellular uptake of siRNA duplexes following noncovalent packaging with protein transduction domain peptides. Adv. Drug Deliv. Rev. 2008; 60:530–536. [PubMed: 18155315]
11. Bevilacqua PC, Cech TR. Minor-groove recognition of double-stranded RNA by the double-stranded RNA-binding domain from the RNA-activated protein kinase PKR. Biochemistry. 1996; 35:9983–9994. [PubMed: 8756460]
12. Tian B, Bevilacqua PC, Diegelman-Parente A, Mathews MB. The doublestranded-RNA-binding motif: interference and much more. Nat. Rev. Mol. Cell Biol. 2004; 5:1013–1023. [PubMed: 15573138]
13. Ryter JM, Schultz SC. Molecular basis of double-stranded RNA-protein interactions: structure of a dsRNA-binding domain complexed with dsRNA. EMBO J. 1998; 17:7505–7513. [PubMed: 9857205]
14. Boyer LA, et al. Core transcriptional regulatory circuitry in human embryonic stem cells. Cell. 2005; 122:947–956. [PubMed: 16153702]
15. Henderson JK, et al. Preimplantation human embryos and embryonic stem cells show comparable expression of stage-specific embryonic antigens. Stem Cells. 2002; 20:329–337. [PubMed: 12110702]
16. Hay DC, Sutherland L, Clark J, Burdon T. Oct-4 knockdown induces similar patterns of endoderm and trophoblast differentiation markers in human and mouse embryonic stem cells. Stem Cells. 2004; 22:225–235. [PubMed: 14990861]
17. Judge AD, et al. Design of noninflammatory synthetic siRNA mediating potent gene silencing in vivo. Mol. Ther. 2006; 13:494–505. [PubMed: 16343994]
18. Zhang W, et al. Inhibition of respiratory syncytial virus infection with intranasal siRNA nanoparticles targeting the viral NS1 gene. Nat. Med. 2005; 11:56–62. [PubMed: 15619625]
19. Safran M, et al. Mouse reporter strain for noninvasive bioluminescent imaging of cells that have undergone Cre-mediated recombination. Mol. Imaging. 2003; 2:297–302. [PubMed: 14717328]

20. Miyoshi H, et al. Development of a self-inactivating lentivirus vector. J. Virol. 1998; 72:8150–8157. [PubMed: 9733856]

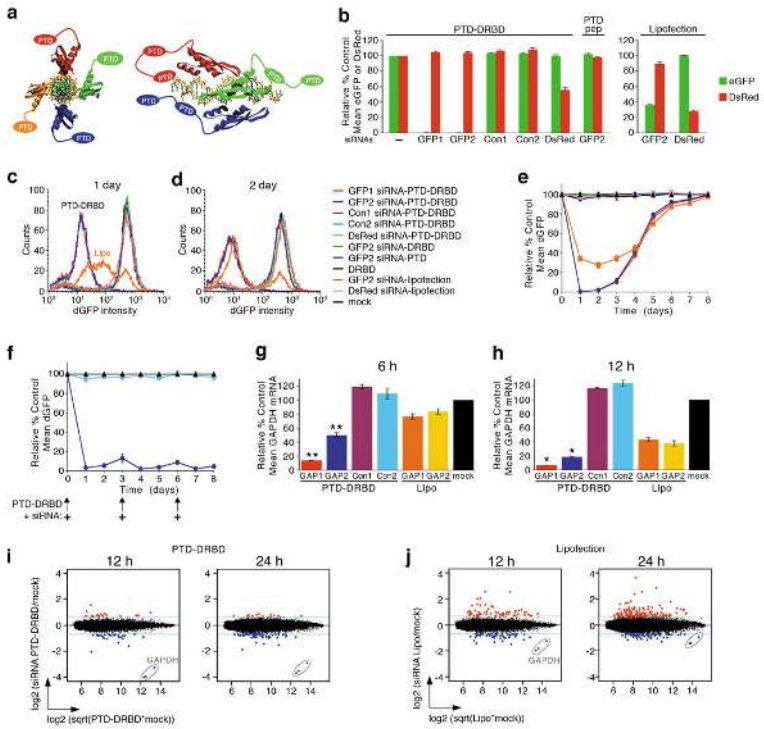

Figure 1. PTD-DRBD mediated siRNA delivery

(**a**) Hypothetical cartoon of PTD-DRBD bound to siRNA. DRBD Ribbon structure derived from Ryter and Schultze13 (**b**) Normalized RNAi knockdown of dGFP and dDsRed by PTD-DRBD:siRNA (left panel) and lipofection (right panel), as indicated, in H1299 dGFP/dDsRed cells. Mean values were normalized to percent control. (**c,d**) Single cell flow cytometry histogram analysis of dGFP RNAi response at 1 and 2 days post-treatment of H1299 dGFP/dDsRed cells, as indicated. (**e**) Flow cytometry analysis of dGFP RNAi knockdown decay kinetics following a single siRNA treatment of dividing H1299 dGFP/dDsRed cells. (**f**) Flow cytometry analysis of dGFP RNAi knockdown decay kinetics following multiple siRNA treatments of H1299 dGFP cells, as indicated. Mean values are normalized to percent control. (**g,h**) Quantitative RT-PCR analysis of endogenous GAPDH mRNA expression at 6 and 12 h post-treatment in H1299 cells, as indicated. Mean values normalized to β2 microglobulin and reported as percent of mock GAPDH control. **(P<0.001) and *(P<0.005) of specific siRNA delivered by PTD-DRBD compared to lipofection. (**i,j**) Whole genome microarray profile M-A plot of GAPDH siRNA delivered by PTD-DRBD (**i**) or Lipofection (**j**) at 12 and 24 h post-treatment in H1299 cells, as indicated. Blue line indicates 1.6x fold up/down change.

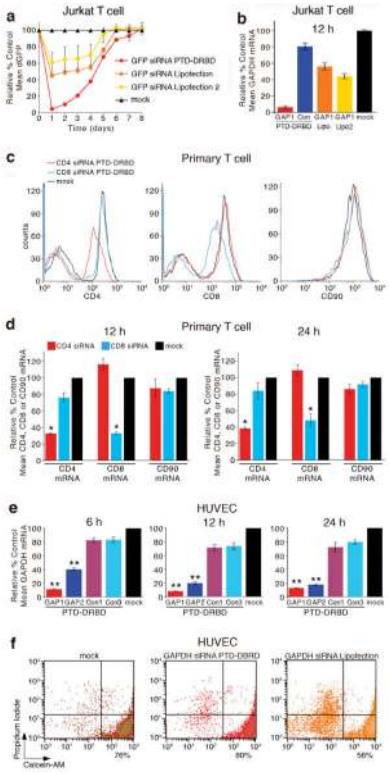

Figure 2. PTD-DRBD siRNA delivery into T cells and HUVECs

(**a**) Flow cytometry analysis of dGFP RNAi knockdown decay kinetics of dividing Jurkat dGFP cells following treatment with GFP2 siRNA plus PTD-DRBD, Lipofection-2000 (Lipofection) or RNAiMAX (Lipofection 2), as indicated. (**b**) Quantitative RT-PCR analysis of endogenous GAPDH mRNA expression at 12 h post-treatment of GAPDH siRNA or GFP2 (Con) siRNA plus PTD-DRBD, GAPDH siRNA plus Lipofection-2000 (Lipofection) or RNAiMAX (Lipofection 2) in Jurkat cells, as indicated. Mean values normalized to β2 microglobulin and reported as percent of mock GAPDH control. (**c**) Flow cytometry histogram analysis of PTD-DRBD mediated CD4 or CD8 RNAi response at 1 day post-treatment of mouse primary T cells, as indicated. (**d**) Quantitative RT-PCR analysis of endogenous CD4, CD8 or CD90 mRNA expression at 12 and 24 h post-treatment of PTD-DRBD CD4 or CD8 siRNAs in primary T cells, as indicated. Mean values normalized to β2 microglobulin and reported as percent of mock control. *($P<0.05$) of specific siRNA vs. control siRNA delivered by PTD-DRBD. (**e**) Quantitative RT-PCR analysis of endogenous GAPDH mRNA expression at 6, 12, and 24 h post-treatment of PTD-DRBD GAPDH or control siRNAs in primary HUVEC cells, as indicated. Mean values normalized to β2 microglobulin and reported as percent of mock GAPDH control. **($P<0.01$) of specific siRNA vs. control siRNA delivered by PTD-DRBD. (**f**) PTD-DRBD cytotoxicity analysis. HUVEC cells were treated with mock (PBS), GAPDH siRNA plus PTD-DRBD or lipofection and analyzed for cytotoxicity by FACS after 24 h post-treatment with two independent means, propidium iodide and Calcein-AM. Percent indicates viable cells present in bottom, right quadrant.

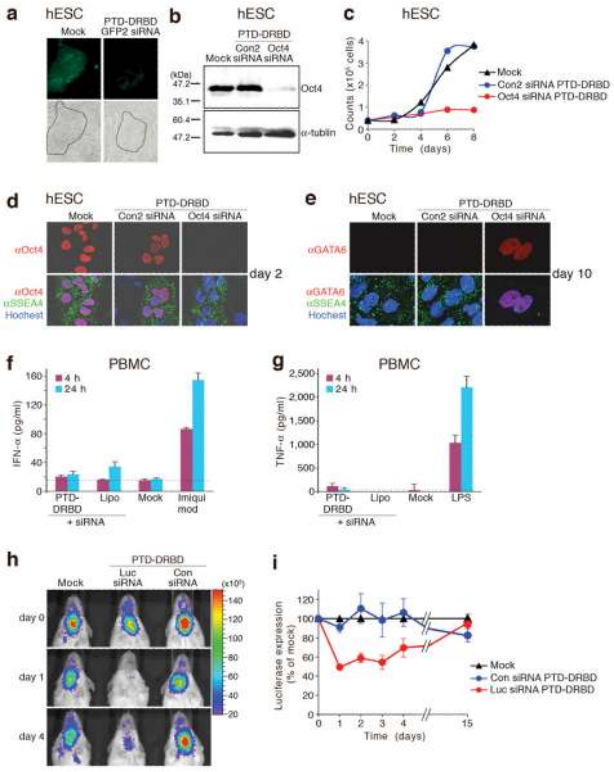

Figure 3. PTD-DRBD mediated RNAi responses

(**a**) Fluorescent microscopy analysis of H9 hESCs constitutively expressing GFP treated with with PTD-DRBD delivered GFP2 siRNA at 2 days post-addition. Black line outlines hESC colony on mouse feeder cell background. (**b**) Oct4 immunoblot analysis in HUES9 hESCs treated with mock (PBS), PTD-DRBD delivered Oct4 or control siRNAs at 2 days post-addition. (**c**) Cell division curve of human HUES9 embryonic stem cells treated with mock (PBS), PTD-DRBD delivered Oct4 or control siRNAs, as indicated. (**d**) Immunohistochemistry analysis of Oct4 and SSEA4 expression in HUES9 hESCs at 2 days post-treatment with mock (PBS), PTD-DRB delivered Oct4 or control siRNAs. Anti-Oct4 antibodies (red), anti-SSEA-4 antibodies (green), genomic DNA (blue). (**e**) Immuno-histochemistry analysis of GATA6 and SSEA4 expression in HUES9 hESCs at 10 days post-treatment with mock (PBS), PTD-DRB delivered Oct4 or control siRNAs. Anti-GATA6 antibodies (red), anti-SSEA-4 antibodies (green), genomic DNA (blue). (**f, g**) Analysis of IFN-α and TNF-α induction in human PBMCs at 4 or 24 h post-treatment with mock (PBS), β-gal siRNA plus PTD-DRBD or plus Lipofection, as indicated. 10 μ/ml Imiquimod Imiquimod or 10 μg/ml LPS was used as a positive control for IFN-α or TNF-α, respectively. (**h**) Nasal and tracheal expressing ROSA26R-Luciferase transgenic mice were live animal imaged on day 0. Randomized groups of luciferase expressing mice were then treated with PBS, PTD-DRBD plus Luc siRNA or control GFP (Con) siRNA and monitored daily for luciferase expression, as indicated. Scale is in photons/s/cm^2/sr. (**i**) Graph of percent Luciferase knockdown mice from (h) above. Luciferase expression was normalized to mock each day, error bar indicates s.e.m., n = 3 for each group with two luciferase readings performed per mouse per day.